PREVENTIVE CONTROL CONSIDERING AGGREGATED CONTROLLABLE LOADS FOR VOLTAGE STABILITY IN ELECTRICAL POWER SYSTEMS

S.H. LI[1,2*], Y. HE[1], H. LI[1,2], H.M. PENG[1]

Aggregated controllable load (ACL) has great potential in power system stability control and ancillary services. This paper proposes a new voltage stability constrained optimal power flow (VSC-OPF) model to coordinate ACL and the other control actions, such as generator terminal voltage adjusting, transformer tap regulation and power generation rescheduling. ACL is recognized as a new control stage to integrate into the proposed VSC-OPF. The successive linear programming method is applied to solve the proposed VSC-OPF. Finally, the effectiveness of the proposed method was verified in the reduced model of Guangzhou power network.

Keywords: voltage stability; demand-response; preventive control; optimal power flow

1. Introduction

With the rise of the electric load and amplitude of renewable generation, the modern power system is more likely to operate closer to its physical limits [1]. Therefore, blackout events caused by voltage collapse occurred more frequently in recent decades, which seriously affected residents' lives, industrial production, and other aspects of society. To address this problem, advanced preventive control methods to prevent voltage instability are more urgently needed [2]-[3].

Until now, preventive control problem of voltage stability is expressed as the optimal model in the most of publications. The objectives of the optimization models contain two types, one is to maximize voltage stability margin [4]-[5], the other is to minimize the total control costs of voltage regulation actions [6]-[8]. The optimization method adopted the latter type objective is more practical since this method considered all the available voltage regulation actions such as power generation rescheduling, generator terminal voltage adjusting, transformer tap changing, reactive power injection and load curtailment. And these voltage regulation actions were divided into three priority control stages in terms of control cost by the optimization method. Thus, the lower cost control actions are preferentially to be employed. However, load curtailment is still often employed to maintain power system security according to this method as the power system

[1] College of Information Engineering, Xiangtan University, Xiangtan 411105, China
[2] Innovation Center for Wind Power Equipment and Energy Conversion, Xiangtan 411101, China

was operating at tension state, which usually cause large number of losses of the social production once employed.

To reduce the total amount of shed loads, the ability of smart appliances responding to the system demand without sacrificing the comfort of their owners are developed by the researchers in recent years [9]. It is a more grid-friendly and great potential control resource for preventive control. In this context, virtual power plant (VPP) technology is proposed to aggregate these distributed controllable loads (i.e. ACL) to exploit this resource [10]-[11]. VPP technology give ACL the possibility to balance the unexpected power fluctuations and shift peak and mitigate system instability [12]. Literature [13]-[14] propose new control strategies to schedule the optimal capacities of ACL to provide the power system ancillary services. In [15], a real time decentralized voltage control method has been proposed to raise the remote nodal end voltage of the low power networks by controlling the active and reactive consummation of ACL [16]-[17]. A resilient control strategy is established to prevent voltage instability by use of thermostatically controlled loads (TCL) in [18]. However, ACL consists of several components such as TCL, deferrable loads (DL) and plug-in electrical vehicles (PEV) etc., but only few publications refer to use one of them for the preventive control. Moreover, the coordination challenge of ACL control with other control actions for preventive control of voltage stability has not been considered.

In this context, a new VSC-OPF model is proposed to coordinate ACL with other conventional controls in this paper, which is to fully use the potential capacity of ACL in the power system. TCL, DL and PEV are taken account in ACL. The aggregated TCL, DL and PEV models are applied to determine their controllable regions. In the proposed VSC-OPF model, ACL is integrated as a new stage. Then, the successive linear programming method is applied to solve the optimal problem, which considers the lower boundaries of ACL and the evaluation of voltage stability margin (VSM). This method is tested in the reduced Guangzhou power network to verify its effectiveness.

2. Model of Aggregated Controllable Load

TCL mainly consist of air conditioning, ventilation, heating, water heaters and refrigerator. There are the devices which maintain the temperature in the set temperature range of electrical appliances. On the peak load period, the start and stop time of TCL can be controlled or the set temperature can be adjusted to achieve load reduction. The aggregate TCL are often modeled as a one-dimensional equivalent thermal parameter [20] as follows:

$$P_H(t) = \sum_{i=1}^{N} P_h(i,t) \int_{-\infty}^{+\infty} \phi_1(t,\theta) d\theta = P_{H.cap} \Phi(t) \tag{1}$$

where ϕ_1 is the active power-states, which is got from the real-time direct measurement; $P_{H.cap}$ is the installed power of TCLs; $\Phi(t)$ is the capacity-factor at the time t, which can be obtained as a function of the temperature set-point location according to [20]. N is the population of TCLs; $P_h(i,t)$ is the real power consumption of each unit.

In practical experience, the set-point modulations are limited within the quarter-deadband to avoid rapid switching nearby the set temperature [20]. So the feasible region of TCL has to be constrained by :

$$\begin{cases} P_H^*(i,t+\Delta t) \geq P_{TCL}^+(i+\Delta t) \\ P_{H,cap}\Phi(m_{s,\min},t+\Delta t) = P_{TCL}^+(i,t+\Delta t) \\ P_H^*(i,t+\Delta t) \leq P_{TCL}^-(i,t+\Delta t) \\ P_{H,cap}\Phi(m_{s,\max},t+\Delta t) = P_{TCL}^-(i,t+\Delta t) \end{cases} \tag{2}$$

where $P_H^*(t+\Delta t)$ is the available capacity of TCLs at a time interval $t+\Delta t$ considering without compromising end-service; $P_{TCL}^+(i,t+\Delta t)$ and $P_{TCL}^-(i,t+\Delta t)$ is the lower and upper boundaries of the controllable region, respectively. The maximum $m_{s,max}$ and minimum $m_{s,min}$ temperature set-point indices can be obtained by solving the minimization problem proposed in [20].

DL mainly consists of laundry machines, clean dishes and the pool pump, which can shift the power consumption without interrupting the load. In general, the working interval (D) of DL is usually a deterministic function of the machine working program. Thus, the activation of a DL as a known nonhomogeneous Poisson process with arrival rate $\lambda(t)$ based on the conclusion of the statistical properties analysis of the aggregate DL as refered in [21]. By considering the joint probability to have k departures and $i-b+k$ arrivals in $[t,t+\Delta t]$, the conditional probability to have i active users can be expressed as:

$$p_i(t+\Delta t|b) = e^{-\bar{\lambda}_{\Delta t}^t \Delta t} \sum_{k=1}^{b} d_k(t,\Delta t|b) \frac{(\bar{\lambda}_{\Delta t}^t \Delta t)^{i-b+k}}{(i-b+k)!} \tag{3}$$

Assuming the average capacity is constant in the next time interval, so the total capacity expectation of the aggregate DL at $[t,t+\Delta t]$ is estimated by:

$$P_{DL}(t+\Delta t) = \sum_{j=1}^{b(t+\Delta t)} j \times p_j \times q_{av} \tag{4}$$

The average power consumer q_{av} is obtained by $q_{av} = P_{DL}(t)/b(t)$ [22]. Thereby, the feasible region of the aggregate DL is constrained within:

$$0 \leq \Delta P(t+\Delta t) \leq P_{DL}(t+\Delta t) \tag{5}$$

Normally, PEV operates at three different modes, namely disconnected, idle, and charging. The participation factor and state-of-capacity (SOC) of PEVs are known in terms of the real operating state of the PEVs. The upper and lower boundaries of SOC are pre-set to avoid battery over discharge and overcharge [23]-[24]. The power of electric vehicle fleets can be aggregated into one large source model based on the participation factor, which facilitates the incorporation of several PEV fleets characteristics such as minimum desired state of charge (SOC) of the PEV owners, drive train power limitations, charging modes of PEVs as referred in [24]. The total upward ΔP_{ag}^{+} and downward ΔP_{ag}^{-} reserves of N_h number of PEVs aggregate model can be obtained by:

$$\begin{cases} \Delta P_{ag}^{+} = \sum_{i=1}^{N_h} m_i \cdot (P_i^{\max} - P_{c,i} - \Delta P_{sev,i}) \\ \Delta P_{ag}^{-} = \sum_{i=1}^{N_h} m_i \cdot (P_{c,i} + \Delta P_{sev,i} - P_i^{\min}) \end{cases} \tag{6}$$

where P_c is the sum of charging power; ΔP_{sev} is the sum power for other service, for instance, frequency control; $P^{\max}, P^{\min}$ is the drive train maximum and minimum power limit.

3. The proposed VSC-OPF for preventive control

3.1 The proposed VSC-OPF model

According to the conventional VSC-OPF model [15], the control actions are often divided into the three priority stages in term of control cost. The larger number of the stage correspond to the higher control cost. Thus, the previous stage is effective, the latter stage should be avoided in the conventional VSC-OPF. On the basis of that, ACL can be recognized as a new stage to integrate it into the new VSC-OPF. The proposed VSC-OPF model for preventive control of voltage stability is expressed as follows :

$$\begin{aligned} \min Z_1 &= \sum_{i=1}^{n_{stage}} w_i \sum_{j=1}^{n_i} \left(c_j^{+} \Delta \mu_j^{+} + c_j^{-} \Delta \mu_j^{-} \right) \\ s.t. \quad & F(x, \lambda, \mu) = 0 \\ & 0 \le \Delta \mu_j^{+} \le \mu_j^{\max} - \mu_j^{0} \\ & 0 \le \Delta \mu_j^{-} \le \mu_j^{0} - \mu_j^{\min} \\ & \sum_{j=1}^{n_g} \left(\Delta P_j^{+} - \Delta P_j^{-} \right) = 0 \\ & \lambda_0 + \sum_{i=1}^{n_{cont}} \frac{d\lambda_{\max}}{d\mu_i} (\Delta \mu_i^{+} - \Delta \mu_i^{-}) \ge \sigma \lambda_{rep} \end{aligned} \tag{7}$$

where F is the power flow equation; $\Delta\mu_j^+$, $\Delta\mu_j^-$ is the turn up and down control variable; c_j^+ , c_j^- is the corresponding incremental, decremental control cost, respectively; n_{stage} is number of stage of control measures; w_i is weight factor of ith stages of control, which is set to reflect the priority of control measures; $\Delta P_j^+, \Delta P_j^-$ is the turning up and down power generation [18].

The forth equation of (7) indicates the variation of the system active power consumer and supply should always maintains equal in case of the network active loss is balanced by slack bus. The last equation of (7) indicates the security inequality constraint to reserve a certain level of VSM for all critical contingencies, n_{cont} is the number of the selected controllable measures; λ_{rep} is the desired minimum LM; λ_0 is the initial value of LM, which is obtained by continuation power flow (CPF); σ is an adjustment factor, which is given by the system operator in term of the operation situation, it is set to 1.05 in this paper. $d\lambda_{\max}/d\mu_i$ is the sensitivity of LM with respect to control variables, which are obtained based on the Look-Ahead method [25].

In this proposed model, the control cost of ACL is determined with considering the tradeoff between the practical costs and incentivize affection of the dispatch. Many pricing strategies, such as real time pricing (RTP), time of use (TOU) pricing, and critical peak pricing (CPP) have been investigated [26]-[28]. RTP is a premise method from the perspective of consumer. However, dealing with so many bids of ACL in the process of optimization algorithm for preventive control is impractical. To match the sampling rule of load demand (each day is divided into a certain number of intervals), the TOU pricing strategy is adopted to determine the electricity price in this paper. And then, the defining control cost of ACL is equal to τ times of the real-time price of electricity:

$$c_{vpp}(t) = \tau p_{real}(t) \qquad \tau \geq 1 \tag{8}$$

where c_{vpp} is the control cost; τ is a weight coefficient decided by Grid EMS, in consideration of the electricity of PEV purchase from utility, $\tau \geq 1$, here is set to 1.5; p_{real} is the electricity price in real time, which is set as a constant value 0.12$ according to the reference [28].

The control cost of ACL is higher than generator active power rescheduling, but lower loss than load curtailment. Thus, a new stage (the 3rd stages μ''') of ACL is integrated between generator active power rescheduling and load curtailment. n_{stage} increase from 3 to 4 in the above model (7), (i.e. n_{stage}=1, 2, 3, 4). Based on (2), (5) and (6), the feasible region is obtained to constraint the

new control variable from ACL. For non-negativity purposes, the new control variable is decomposed into:

$$\begin{cases} \mu''' = \Delta P_{ACL}^{+} - \Delta P_{ACL}^{-} \\ 0 \le \Delta P_{ACL}^{+} \le P_{TCL}^{+}(t+\Delta t) + P_{DL}(t+\Delta t) \\ \qquad\qquad + \Delta P_{ag}^{+} - P_{TCL}^{0} \\ 0 \le \Delta P_{ACL}^{-} \le P_{TCL}^{0} - P_{TCL}^{-} + \Delta P_{ag}^{-} \\ \Delta P_{ACL}^{+}, \Delta P_{ACL}^{-} \ge 0 \end{cases} \tag{9}$$

where ΔP_{ACL}^{+}, ΔP_{ACL}^{-} is the turn up and down control variable from ACL. P_{ACL}^{0} is the original value of ACL [18].

3.2 Successive Linear Programming Algorithm

The above VSC-OPF is a convex and multidimensional nonlinear OPF problem. This paper adapts the successive linear programming algorithm (SLPA) to solve it, which has an advantage over correcting the errors through the derivative with respect to the discrete control variables, the lower boundaries of ACL and the evaluation VSM etc. Fig.1 shows the algorithm flowchart of the proposed method.

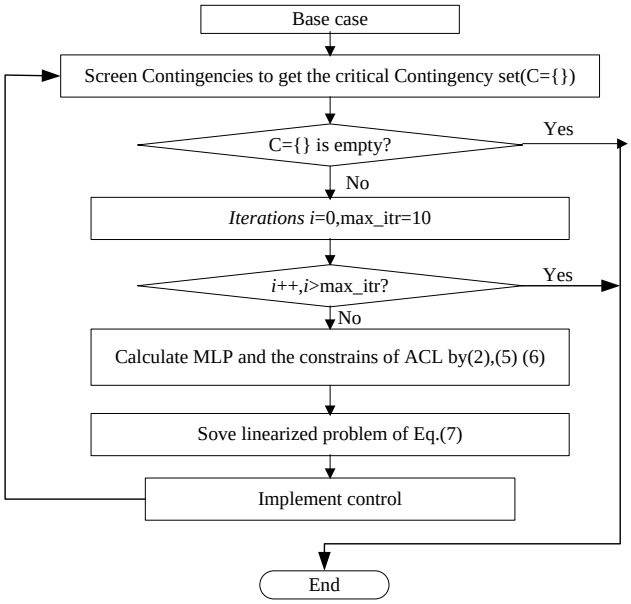

Fig. 1. The flowchart of SLPA

Step 1: Grid EMS reads the real-time data from SCADA including the load level and the power-state information of ACL. Virtual SCADA calculates and sends the controllable region of ACL and its control cost to Grid EMS.

Step 2: Based on the security criterion *N*-1, these contingencies are chosen into the pending contingency set $C=\{\ \}$ whose VSMs are less than the desired minimum threshold. And the control sensitivities are achieved and then rank them;

Step 3: Use linprog function of MATLAB toolbox to solve proposed linear programming model while updating the constraints (7) and using the sensitivity obtained in Step 2 as well as the feasible region defined by (9) that has been obtained from load aggregation.

Step 4: Update state and repeat Step 1, the maximum iteration time *i* is set as 10. If pending contingency set is not empty, continue to Step 2. Otherwise, the preventive control computation is pursued.

4. Case study

The proposed method has been tested on the reduced model of Guangzhou 220 kV power network in the south of China, to verify its effectiveness. The time-domain simulation data is obtained by BPA-PSD (power system integrated simulation software). The simulation is run on a PC with Intel(R) Core i7-3770, 3.40 GHz processor with 16 GB of RAM, a series of data are collected every half hour in a day's time (48 samples in total).

4.1 The reduced Guangzhou 220 kV power network

The reduced Guangzhou 220 kV power network composed of 59 buses and 107 lines. 11 distributed generators and 51 load groups are connected to the network buses. We assume each load group contains both the conventional load and the ACL from large scale VPP which can be dispatched as virtual generation. The capacity of TCLs and DLs is assumed 10 and 5 percent of the current resident load of each load group. The capacity of PEVs is equal to the capacity of DLs and the capacity of the individual PEVs fleet is 5 MW. The operating data of this case is given based on a typical daily operation scenario at the summer of 2015.The daily load curve is predefined as shown in Fig. 2.

As shown in the Fig. 2, we can find the peak demand appeared in the two periods: (A) 12:00-15:00 and (B) 18:30-20:00. In the period A, the active power demand peak reached to 1820.2 MW and reactive power reaches to 865.6 MVAr at about 13:00. During this period, LM is observed to be close to the minimum security threshold which was set as $\lambda_{req}=0.05$ by WECC.

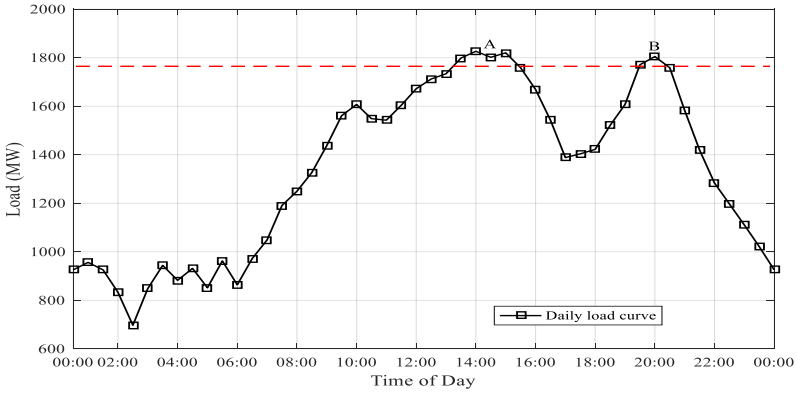

Fig. 2. The daily active power demand curve

Nevertheless, other levels of security margin threshold could be easily adopted. The system may have insufficient LM once a contingency occurred, even become unstable directly.

The security criterion *N*-1, a list of 107 preconceived contingencies while only considering lines outage, is analyzed at the research time to select the critical contingencies. Table 1 list the 7 critical contingencies at the time 13:00, at this time, the power system reaches the top load level. The LMs of all 7 critical contingencies are less than 0.05.

Table 1

Contingency Analysis Result

Classify	Case ID	Outage Lines	At 13:00
	Normal	No contingency	0.0661
Emergency contingency	C096	Guannan-Huqiao	-0.0153
	C142	Zhujianga-Niaozhou	-0.0108
Critical contingency	C113	Beijiao-Shijing	0.0153
	C037	Huadi-Ganling	0.0180
	C060	Fushan-Shiyang	0.0331
	C086	Houde-Boluo	0.0440
	C105	Chisha-Huapu	0.0462

As shown in Table 1, the emergency contingencies C096 and C142 have the negative value of LM, which implies that the system loses stability in case of the two contingencies occurred. Such serious contingencies are more suitable for emergency control strategy rather than preventive control [29]. Thus, these scenarios are not analyzed in this paper.

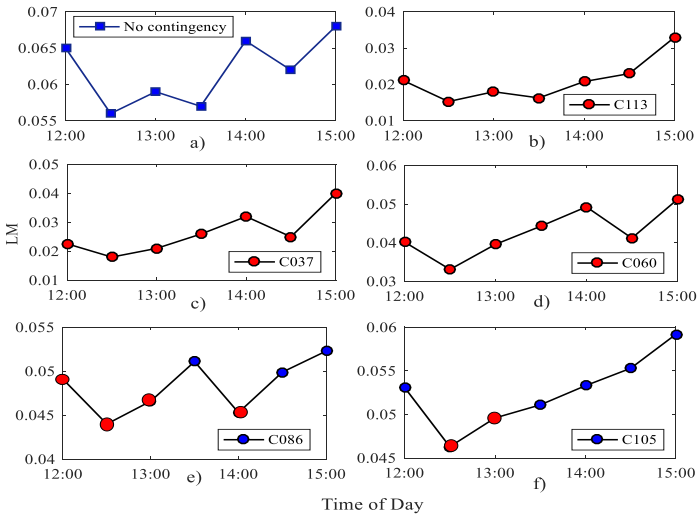

Fig. 3. VSM obtained for the system without access to the proposed control strategy over period A

Fig.3 plots the LM trajectory in the period A without implement the preventive control. Fig.3 (a) is the LM trajectory without contingency. Fig.3 (b)-(h) depict the LMs under the critical contingency C113, C037, C060, C086 and C105. The results demonstrate that the LM cross the given security margin threshold during this period. LMs obtained during the period A of the contingency C113, C060 and C037 are all less than 0.05, as the red dots in Fig.3. This situation implies the system has insufficient stability margin during the period A. Thereby, the contingency protocols are needed to maintain voltage stability.

4.2 Simulation results

For voltage control, this system has 8 available shunt capacitors (which belong to stage 1, each capacitor has 30 Mvar available capacity), 2 generators (which belong to stage 2, Zhujiang and Huapu have regulating capacity 80 and 50 MW) and 29 loads (which belong to stage 3 and 4) were considered as control variables. The proposed control strategy given by (14) is used to make the contingency protocols for this system. In this paper, communication delays for aggregation are not considered.

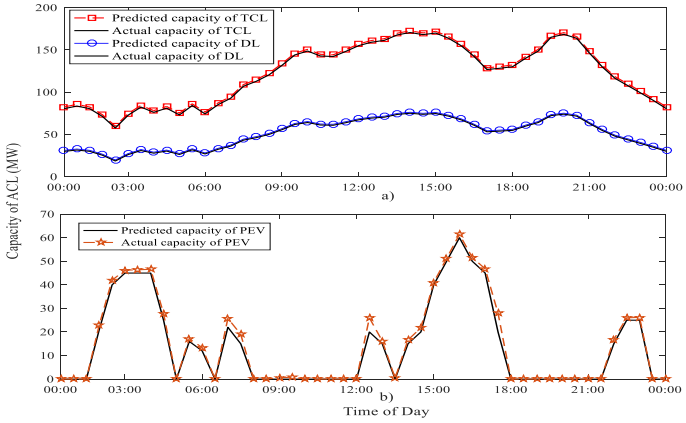

Fig. 4. The actual and predicted capacity of ACL: a) TCL and DL, b) PEV

According to the aggregated models of TCL, DL and PEV, the predicted capacity of TCL, DL and PEV can be obtained by (2), (5) and (6), respectively. The necessary parameters for the calculation of the controllable region of TCL, DL and PEV are referred in [20], [21] and [24], the set values of their case studies are used. Fig.4 shows the comparison of the actual value and the predicted capacity of ACL. From the Fig.4, we can see the predicted curve is very close to the actual curve, in fact, the errors between the actual values and the predict value are less than 2%. Therefore, the controllable regions based on the capacity obtained by the proposed models are feasible.

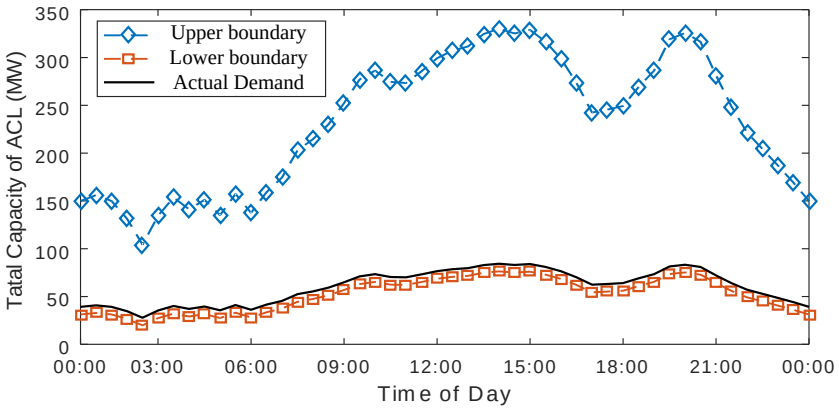

Fig. 5. The controllable regions and actual demand of ACL

After computing the predicted capacity, the total controllable regions of ACL are calculated by (15) before the optimization procedure. Fig.5 summarizes the controllable regions that ACL is dispatched to maintain voltage stability. The

upper and lower boundaries of ACL are achieved by Virtual SCADA and sent to Grid EMS. Then, Grid EMS obtained the actual demand for preventive control by solving the optimization function Z_1. The actual demand is translated as an order signal and sent to Virtual SCADA. In fact, ACL model parameters are varied following the changes of the power-states, so the lower and upper boundaries are time-varied and updated to constrain the available regions of ACL as the Fig. 5. shown. Considering this constraint, the Virtual SCADA determines the specific number and location of controls in term of control sensitivity and cost of control variables. Based on the look-ahead method, Table 2 lists the rank of sensitivity of LM with respect to the control variables of ACLs at the partral buses. See Table 2, load curtailment of bus KAIXUAN have the most effect on improving system stability, so the load of bus KAIXUAN is prior to be selected in the preventive control scheme.

Table 2

Results of Sensitivity LM with respect to ACL in Period A

Time of Day	Sensitivity					
	KAIXUAN	LISHA	CHISHA	SHIJING	HUADI	HOUDE
12:00	0.06361	0.06248	0.06169	0.06118	0.06004	0.05921
12:30	0.06465	0.06309	0.06255	0.06179	0.06120	0.06089
13:00	0.05992	0.05935	0.05912	0.05895	0.05833	0.05632
13:30	0.06225	0.06116	0.06025	0.05986	0.05968	0.05893
14:00	0.05961	0.05922	0.05890	0.05822	0.05808	0.05766
14:30	0.05939	0.05876	0.05839	0.05816	0.05784	0.05734
15:00	0.05902	0.05856	0.05746	0.05762	0.05709	0.05644

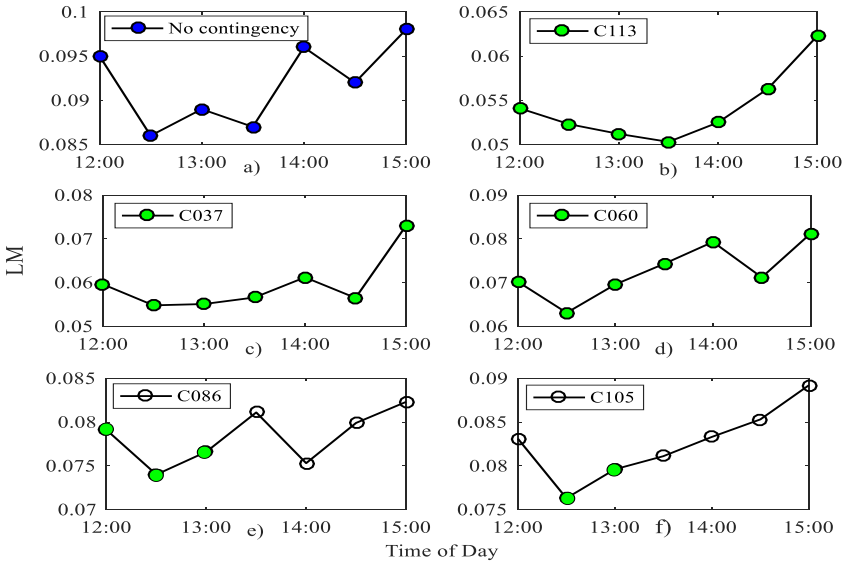

Fig. 6. VSM obtained for the system with access to the proposed control strategy over period A

The control weights are 1, 2, 5, and 10, respectively. The results of the controllable regions, sensitivities and costs are sent to Virtual SCADA, where these parameters and constraints are used to define the nodal load-shedding requirement based on the VSC-OPF given by Z1. In Fig.5, the actual demand level consistently lies near the lower feasible region boundary as the system has restored a certain security level. Finally, the control signals are sent to controllable loads to achieve the control scheme. Fig.6 (a)-(f) depicts the VSMs in the period A after application of the optimal preventive control.

As shown in Fig.6, after application of the selected preventive controls, LMs are observed to be reserved over the security margin threshold 0.05 for all critical contingencies. The all red dots are changed to green color which means VSM is larger than 0.05. The above analysis demonstrated the feasibility of the proposed method. Further, to evaluate the advantages of the proposed method, the conventional VSC-OPF proposed in [7] is tested in the same power network. Table 3 lists the results obtained by the conventional strategy and the proposed strategy.

As shown in Table 3, the strategy decided by SLPA needs 120 MW of shunt capacitors and ±50 MW rescheduling generators output powers to participate in the preventive control. '+' denotes the increase of output power, '-' is reversed, and they always are equal. The minimum load curtailment needs 40 MW. Comparing with the conventional method, less capacity of shunt capacitors and generators are used in the proposed strategy, it is beneficial to provide more reserve capacities for the operation behind. Moreover, though the larger number of loads (40MW) is cut off in terms of the proposed strategy, the control cost 2635 $ is less than the conventional strategy 3021 $. The main reason is that the ACL is integrated into the proposed optimization model in this paper have considered the end-user comfort and these ACLs are voluntary to be controlled in case of the economic requirements of them were met by the utility. Thus, the control cost (stage 3) composed of the control action price and the following loss of consumers is lower than the undifferentiated load shedding (stage 4). The proposed method contributes to achieve the effective decision of preventive control.

Table 3

Comparison of the Optimal Control Scheme obtained by the Conventional and Proposed Strategies

Strategy	Optimal control scheme (MW)				Cost ($)
	stage1	stage2	stage3	stage4	
The conventional strategy	160	±90	0	35	3021
The proposed strategy	120	±50	40	0	2635

Table 4 lists the control variables were selected in the iteration process for the optimal preventive controls. Table 4 shows these lower cost controls were utilized as much as possible in the first iteration, so all the capacity of shunt capacitors and generators controllable power are ran out, the minimum security margin constraint (9) was satisfied until the 35 MW (the lower boundary of ACL at this moment) ACL is curtailed. But after application of this scheme, the VSM under C113 contingency reached 0.068, which exceeded the targets (0.05) a lot. So it implied that the control scheme obtained by Iteration 1 have the problem over control, the main reasons is ACL have the lower boundary of control variable. Thus, the subsequent iteration is to adjust the control variables according to the successive linear programming method to correct the errors, the next iteration determined the final optimal scheme. After application of this scheme, the VSM is 0.055 which is very close to the target 0.05.

Table 4

The list of control variables in process of the proposed preventive control strategy

Control stage	Iteration 1 (MW)	Iteration 2(MW)
Stage 1	180	120
Stage 2	±80	±50
Stage 3	35	40
Stage 4	0	0
VSM under C113	0.068	0.055

5. Conclusion

This paper presents a new VSC-OPF model to coordinate ACL with the other control actions for preventive control of voltage stability. Three components TCL, DL and PEV are taken account into ACL. ACL is recognized as a new control stage to integrate into the proposed VSC-OPF. The proposed method has been tested in a reduced Guangzhou power grid. The simulation results show that the optimal control actions were correctly selected in terms of the lowest cost and bring the system to a secure operation region. The group of the optimal control actions can fully exploit the ability of ACL and reduce the total control cost, simultaneously. SLPA was effective to correct errors derive from the discrete control variables, the lower boundaries of ACL and the evaluation VSM to mitigate over control. In addition, SLPA has a lower computational cost, which takes approximately 70 percent time of the conventional method in the premise that ignored the collection time of the real-time power-state of ACL. Therefore, the deployment of the control optimization scheme is more suitable for real time operation.

REFERENCES

[1]. *K. T. Vu, C. C. Liu, C. W. Taylor, and K. M. Jimma*, "Voltage instability: Mechanisms and control strategies," Proc. IEEE, **vol. 83**, no. 11, pp. 1442–1455, Nov. 1995.

[2]. *T.Van Cutsem*, "Voltage instability: phenomena, countermeasures, and analysis methods," Proceedings of the IEEE, **vol. 88**, no. 2, pp. 208-227, Feb. 2000.

[3]. *K. T. Vu, C. C. Liu, C. W. Taylor, and K. M. Jimma*, "Voltage instability: Mechanisms and control strategies," Proc. IEEE, **vol. 83**, no. 11, pp. 1442–1455, Nov. 1995.

[4]. *Zhihong Feng, V. Ajjarapu and D. J. Maratukulam,* "A comprehensive approach for preventive and corrective control to mitigate voltage collapse," in IEEE Transactions on Power Systems, **vol. 15**, no. 2, pp. 791-797, May 2000.

[5]. *E. De Tuglie, M. La Scala, and P. Scarpellini,* "Real-time preventive actions for the enhancement of voltage-degraded trajectories," IEEE Trans. Power Syst., **vol. 14**, no. 2, pp. 561–568, May 1999.

[6]. *Mansour, M.R.; Alberto, L.F.C.; Ramos, R.A.,* "Preventive Control Design for Voltage Stability Considering Multiple Critical Contingencies," IEEE Transactions on Power Systems, **vol.PP**, no.99, pp.1-9, 2015

[7]. *Capitanescu F; Cutsem T V,* "Preventive control of voltage security: A multi-contingency sensitivity-based approach," IEEE Trans on Power Systems, vol.17, no.2, pp:358-364, 2002

[8]. *M. R. Mansour, L. F. C. Alberto and R. A. Ramos,* "Preventive Control Design for Voltage Stability Considering Multiple Critical Contingencies," IEEE Transactions on Power Systems, **vol. 31**, no. 2, pp. 1517-1525, March 2016.

[9]. *S. Massoud Amin and B. F. Wollenberg,* "Toward a smart grid: power delivery for the 21st century," IEEE Power and Energy Magazine, **vol. 3**, no. 5, pp. 34-41, Sept.-Oct. 2005.

[10]. *Molderink A, Bakker V, Bosman M, Hurink J, Smit G.* Management and control of domestic smart grid technology. IEEE Trans Smart Grid 2010;1:109–19.

[11]. *M. Giuntoli and D. Poli,* "Optimized Thermal and Electrical Scheduling of a Large Scale Virtual Power Plant in the Presence of Energy Storages," IEEE Transactions on Smart Grid, **vol. 4**, no. 2, pp. 942-955, June 2013.

[12]. *E. G. Kardakos, C. K. Simoglou and A. G. Bakirtzis,* "Optimal Offering Strategy of a Virtual Power Plant: A Stochastic Bi-Level Approach," IEEE Transactions on Smart Grid, **vol. 7**, no. 2, pp. 794-806, March 2016

[13]. *Y. Wang, X. Lin and M. Pedram,* "A Near-Optimal Model-Based Control Algorithm for Households Equipped With Residential Photovoltaic Power Generation and Energy Storage Systems," IEEE Transactions on Sustainable Energy, **vol. 7**, no. 1, pp. 77-86, Jan. 2016.

[14]. *J. L. Mathieu, S. Koch, and D. S. Callaway,* "State estimation and control of electric loads to manage real-time energy imbalance," IEEE Transactions on Power Systems, **vol. 28**, no. 1, pp. 430 –440, Feburary 2013.

[15]. *Mufaris, A.L.M.; Baba, J.; Yoshizawa, S.; Hayashi, Y.* "Dynamic voltage regulator operation with demand side management for voltage control", Power Tech, 2015 IEEE Eindhoven, On page(s): 1 – 6

[16]. *J. Yi et al.,* "Distribution network voltage control using energy storage and demand side response," 2012 3rd IEEE PES Innovative Smart Grid Technologies Europe (ISGT Europe), Berlin, 2012, pp. 1-8.

[17]. *I. D. de Cerio Mendaza, I. G. Szczesny, J. R. Pillai and B. Bak-Jensen,* "Flexible Demand Control to Enhance the Dynamic Operation of Low Voltage Networks," IEEE Transactions Smart Grid, **vol. 6**, no. 2, pp. 705-715, March 2015.

[18]. *D. Wang, S. Parkinson, W. Miao, H et al.*, Online voltage security assessment considering comfort-constrained demand response control of distributed heat pump systems, Applied Energy, Volume 96, August 2012, Pages 104-114.

[19]. *Callaway D, Hiskens I*. Achieving controllability of electric loads. Proc IEEE 2011;99:184–99.

[20]. *Callaway D*. Tapping the energy storage potential in electric loads to deliver load following and regulation, with application to wind energy. Energy Convers Manage 2009;50:1389-400.

[21]. *S. P. Meyn, P. Barooah, A. Bušić, Y. Chen and J. Ehren,* "Ancillary Service to the Grid Using Intelligent Deferrable Loads," IEEE Transactions on Automatic Control, **vol. 60**, no. 11, pp. 2847-2862, Nov. 2015.

[22]. *S. Pagliuca, I. Lampropoulos, M. Bonicolini, B. Rawn, M. Gibescu, and W. L. Kling*, "Capacity assessment of residential demand response mechanisms," Universities' Power Engineering Conference (UPEC), Proceedings of 2011 46th International, 2011, pp. 1–6.

[23]. *S. Izadkhast, P. Garcia-Gonzalez and P. Frías,* "An Aggregate Model of Plug-In Electric Vehicles for Primary Frequency Control," IEEE Transactions on Power Systems, **vol. 30**, no. 3, pp. 1475-1482, May 2015

[24]. *S. Izadkhast, P. Garcia-Gonzalez, P. Frìas, L. Ramìrez-Elizondo and P. Bauer*, "An Aggregate Model of Plug-in Electric Vehicles Including Distribution Network Characteristics for Primary Frequency Control," IEEE Transactions on Power Systems, **vol. 31**, no. 4, pp. 2987-2998, July 2016.

[25]. *Reda Mansour, M.; Geraldi, E.L.; Costa Alberto, L.F.; Andrade Ramos, R.*, "A New and Fast Method for Preventive Control Selection in Voltage Stability Analysis," IEEE Transactions on Power Systems, **vol.28**, no.4, pp.4448-4455, Nov. 2013

[26]. *M. Muratori and G. Rizzoni*, "Residential Demand Response: Dynamic Energy Management and Time-Varying Electricity Pricing," IEEE Transactions on Power Systems, **vol. 31**, no. 2, pp. 1108-1117, March 2016.

[27]. *Katipamula S, Chassin D, Hatley D, Pratt R, Hammerstrom D*. Transactive controls: Market-based GridWise controls for building systems, Prepared for the US Department of Energy under Contract DE-AC05-76RL0183 PNNL-15921; 2006.

[28]. *J. H. Yoon, R. Baldick and A. Novoselac*, "Dynamic Demand Response Controller Based on Real-Time Retail Price for Residential Buildings," IEEE Transactions on Smart Grid, **vol. 5**, no. 1, pp. 121-129, Jan. 2014.

[29]. *M. Begovic, D. Novosel, D. Karlsson, C. Henville and G. Michel*, "Wide-Area Protection and Emergency Control," Proceedings of the IEEE, **vol. 93**, no. 5, pp. 876-891, May 2005.